Supporting Information

Drazic et al. 10.1073/pnas.1718336115

SI Materials and Methods

Antibodies and Reagents. A detailed list of all plasmid constructs, antibodies, and peptides used in the study is provided in Table S3.

Plasmid Construction, Recombinant Protein Expression, and Purification of hNAA80. *hNAA80/hNAT6* (NCBI gene ID: 24142) was cloned from human HEK 293 cDNA by use of Transcriptor Reverse Transcriptase (Roche) using the following primers: NAA80 sense primer (5′-CAACATGCAAGAGCTGACTC-3′) and NAA80 antisense primer (5′-GATGTCTTTTTCCATCCAGAATATG-3′). The PCR product containing the coding sequence was inserted into the TOPO TA vector pcDNA 3.1/V5-His TOPO (Invitrogen) using the provided kit, resulting in the plasmid pNAA80-V5. Plasmid hNAA80-eGFP was constructed using pNAA80-V5 as the template and restriction sites NheI and KpnI in peGFP-N1. The MBP-His-hNAA80 fusion protein (MBP-NAA80) was constructed by subcloning hNAA80 from the plasmid pNAA80-V5 into the pETM-41 vector using the restriction enzymes NcoI and Acc65I, resulting in pETM-41-hNAA80. The plasmid was transformed into *Escherichia coli* BL21 Star (DE3) cells (Invitrogen) by heat shock. A 300-mL cell culture was cultivated in Luria–Bertani medium at 37 °C until an OD_{600} of 0.6 was reached and subsequently was transferred to 20 °C. Protein expression was induced by the addition of 1 mM isopropyl-β-D-thiogalactopyranoside (IPTG). After 16 h, the cells were harvested by centrifugation, and the pellets were stored at −20 °C. For purification, the *E. coli* pellets were thawed at 4 °C, and the bacterial cells were lysed using mechanical disruption by a French press (1,000 psi pressure) in lysis buffer [50 mM Tris·HCl (pH 8.0), 300 mM NaCl, 20 mM imidazole, 1 mM DTT, 1× EDTA-free protease inhibitor mixture (Roche)]. After centrifugation (40,000 × *g*, 25 min, 4 °C), the cell extract was applied on a metal-affinity FPLC column (HisTrap HP; GE Healthcare). MBP-NAA80 was eluted with 300 mM imidazole in 50 mM Tris (pH 8.0), 300 mM NaCl, and 1 mM DTT. Recombinant protein-containing fractions were pooled and further purified via size-exclusion chromatography (Superdex 200; GE Healthcare), and purity was determined by analysis of Coomassie-stained SDS/PAGE gels. The protein concentrations were determined by absorption at 280 nm using a NanoDrop 1000 spectrophotometer (Peqlab Biotechnologie GmbH).

[^{14}C]-Ac-CoA–Based NAT Assay Using Synthetic Oligopeptides. The assay was performed as described previously (1). Briefly, the immunoprecipitates were mixed with 200 μM selected synthetic oligopeptides (BioGenes) and 50 μM isotope-labeled [^{14}C]-Ac-CoA (Perkin-Elmer) in a total volume of 25 μL acetylation buffer [50 mM Tris (pH 7.4), 1 mM EDTA, 1 mM DTT, 10% (vol/vol) glycerol]. The samples were incubated at 37 °C with shaking at 1,000 rpm in a Thermomixer block for 60 min. The magnetic beads were removed, and the supernatants were transferred onto P81 phosphocellulose filter disks (Millipore). The filter disks were washed three times with washing buffer [10 mM Hepes (pH 7.4)] and dried before they were added to 5 mL Ultima Gold F scintillation mixture (Perkin-Elmer). The incorporated [^{14}C]-Ac was determined by a Perkin-Elmer Tri-Carb 2900TR Liquid Scintillation Analyzer.

DTNB Nt-Acetylation Assay. The 5,5′-dithiobis-(2-nitrobenzoic acid) (DTNB) Nt-acetylation assay was performed as described previously (2). Briefly, purified enzyme (1.5 μM) was mixed with peptides (500 μM) and Ac-CoA (500 μM) in acetylation buffer [50 mM Tris·HCl (pH 8.5), 200 mM NaCl, and 2 mM EDTA] at 37 °C, and reactions were quenched after 30 min with quenching buffer [3.2 M guanidinium-HCl, 100 mM sodium phosphate dibasic (pH 6.8)]. To measure CoA production, DTNB [2 mM final concentration dissolved in 100 mM sodium phosphate dibasic (pH 6.8) and 10 mM EDTA] was added to the quenched reaction. The thiol present in the enzymatic product, CoA, cleaves DTNB and produces 2-nitro-5-thiobenzoate (TNB^{2-}), which is readily quantified by monitoring the absorbance at 412 nm. Background absorbance was determined in negative controls and was subtracted from the absorbance determined in each individual reaction. Thiophenolate production was quantified assuming $\varepsilon = 13.7 \times 10^3$ M/cm.

Human Cell Culture and Transfection. HAP1 cells were obtained from Horizon Genomics and cultured as recommended. HAP1 is a near-haploid human cell line that was derived from the male chronic myelogenous leukemia cell line KBM-7. HAP1 cells are adherent with fibroblast-like morphology and are smaller than most frequently used cell lines. *NAA80*-KO and wild-type HAP1 cells (Horizon C631) were grown in Iscove's Modified Dulbecco's Medium with the addition of 10% FBS and 1% penicillin/streptomycin. Since HAP1 cells typically diploidize spontaneously over time, all HAP1 cell lines were passaged until diploid status was confirmed by an Accuri BD C6 flow cytometer using propidium iodide staining before they were used in experiments. HeLa cells (ATTC CCL-2) were cultured in DMEM/10% FBS at 37 °C and 5% CO_2. Cells were seeded on plates or coverslips and transfected with X-tremeGENE 9 (Roche) as recommended. For localization and phenotype rescue studies, cells were imaged ∼24 h and 48 h posttransfection, respectively.

Wound-Healing/Gap-Closure and Chemotaxis Assays. For wound-healing assays as shown in Fig. 2 *A–C*, cells were seeded in wells of silicone culture inserts (ibidi 80209) placed in slide wells (ibidi 80426). Ninety microliters of 300,000 cells/mL were seeded in each insert well, resulting in 100% confluency after ∼24 h, at which time insets were removed (creating a 400- to 450-μm-wide gap). Wells were washed twice in medium, and time-lapse imaging started using a Nikon TE2000 microscope with 10× objective. ImagePro plus was used for image processing to measure gap size in square micrometers. Cell-front velocity was calculated according to ibidi application note 30. The total area of the image was multiplied with the centerpiece approximation (the percent of increase of the cell-covered area per time unit; this number was divided by the length of the image in micrometers, and the resulting number was divided by 2 for the two cell fronts), resulting in the normalized cell-front velocity expressed in micrometers per hour. For scratch wounds using the IncuCyte ZOOM imaging system, 200 μL of 40,000 cells/mL were seeded in 96-well ImageLock plates (Essen BioScience), and scratch wounds were prepared with the accompanying scratch-wound maker (creating a 700-μm-wide gap) according to the manufacturer's protocols. Wells were washed twice and filled with 300 μL medium. Wounds (two positions per well) were imaged every 2 h for 24 h by IncuCyte scanning. Image analysis was performed using the IncuCyte ZOOM software using area masks for wound- and cell-covered areas and calculations of average gap size. Cell-front velocity was calculated as above. For the chemotaxis assay in the IncuCyte ZOOM, cells were seeded in membrane-containing inserts of ClearView 96-well cell-migration plates with porous membranes. Cells were seeded at a density of 27,000 cells/mL, 60 μL per insert well, in medium containing 1% FBS. After 3 h,

media of different FBS concentrations were added to the appropriate top or bottom wells to obtain the desired final concentrations of FBS while keeping volumes equal. The membranes were imaged at the top and bottom using a 10× objective every 2 h for 24 h. Analysis was performed using the IncuCyte ZOOM software measuring the cell-covered area at the top and bottom. Numbers were expressed as the amount of cells that had migrated per time as a percentage of the initial top value. Data were background-subtracted and corrected for growth differences.

Immunoprecipitation of NAA80-V5. For immunoprecipitation of NAA80-V5, 7.5×10^6 transfected HeLa cells per sample were harvested and lysed in 450 μL of lysis buffer [50 mM Tris (pH 8.0), 150 mM NaCl, 0.1% Nonidet P-40, 1 × EDTA-free protease inhibitor mixture (Roche)] for 15 min at 4 °C. Cell debris was then pelleted by centrifugation (17,000 × *g*, 15 min, 4 °C), and the supernatant was collected and transferred to a new Eppendorf tube. The supernatant was incubated for 4 h at 4 °C with 2 μg anti-V5 antibody (Invitrogen). Then, 25 μL of magnetic Protein A/G beads (Millipore) washed three times in lysis buffer were added to the samples. After incubation for 16 h and three repetitive rounds of washing (two rounds in lysis buffer and one in acetylation buffer; see below), the samples were used in an in vitro [^{14}C]-Ac-CoA peptide acetylation assay.

Isolation of Polysomes. Total ribosome isolation was performed as described previously (3, 4). Briefly, $1.5–2.0 \times 10^7$ HeLa cells were transfected with 1 μg NAA80-V5 for 24 h. Before harvesting, cells were treated with 10 μg/mL cyclohexamide for 5 min at 37 °C. Cells were harvested (2,000 × *g*, 5 min, 4 °C), lysed in 1 mL KCl ribosome lysis buffer [1.1% (wt/vol) KCl, 0.15% (wt/vol) triethanolamine, 0.1% (wt/vol) magnesium acetate, 8.6% (wt/vol) sucrose, 0.05% (wt/vol) Na-deoxycholate, 0.5% (vol/vol) Triton X-100, 0.25% (vol/vol) Pefabloc (Roche)], and incubated on ice for 15 min. Nuclei and membranes were removed by centrifugation at 400 × *g* for 10 min, and 700 μL of cell lysate was centrifuged at 470,000 × *g* for 25 min on a 0.4-mL cushion of 25% sucrose in KCl ribosome lysis buffer using an MLA-130 rotor (Beckman). Pellets were resuspended in ribosome lysis buffer with the indicated KCl concentrations, followed by ultracentrifugation as described above. Pellets were resuspended in KCl ribosome lysis buffer and prepared for analysis by SDS/PAGE and Western blotting.

[^{14}C]-Ac-CoA–Based Nt-Acetylation of Cell Lysates and SDS/PAGE Analysis. HAP1 control and NAA80-KO cells (6×10^7 cells) were harvested, resuspended in homogenization buffer [20 mM Hepes (pH 7.4), 250 mM sucrose, 1 mM EDTA, 1 × EDTA-free protease inhibitor mixture (Roche)], and lysed using an European Molecular Biology Laboratory (EMBL) Cell Cracker (8.010-mm ball). The cell debris was spun down at 3,000 × *g* for 10 min at 4 °C. To each lysate sample (except for the negative control), 5 μM purified MBP-NAA80 and 47 μM [^{14}C]-Ac-CoA were added. Auto-acetylation activity samples of MBP-NAA80 contained homogenization buffer, 5 μM purified MBP-NAA80, and 47 μM [^{14}C]-Ac-CoA. All samples were incubated at 37 °C for 2 h before Laemmli sample buffer was added and then were incubated at 95 °C for 5 min. Proteins were separated by SDS/PAGE, and the SDS-gel vacuum was dried, followed by exposure to a BAS-IP-SR 2040 film (Fuji Photo Film Co. Ltd) for 28 h. The [^{14}C]-acetylated protein signal was developed by Typhoon FLA 9000 (GE Healthcare).

Strong Cation Exchange Enrichment and LC-MS/MS Analysis of N-Terminal Peptides. Strong cation exchange (SCX) enrichment of N-terminal peptides from HAP1 control and *NAA80* KO1 cells was performed as described previously (5). To enable the assignment of in vivo Nt-acetylation (Ac) events, all primary protein amines were blocked at the protein level making use of a *N*-hydroxysuccinimide (NHS) ester of acetic acid encoded with stable heavy isotopes [i.e., NHS ester of $^{13}C_2D_3$-acetic acid (AcDC)]. In this way, it is possible to distinguish between in vivo-acetylated (Ac) and in vitro-acetylated (AcDC) N termini and to calculate the degree of in vivo Nt-acetylation as described below. After trypsin digestion, N-terminally blocked peptides were enriched by SCX, as such peptides will not bind to the SCX resin at low pH. From both samples, ∼2 μg of the resulting peptide mixture was injected for LC-MS/MS analysis on an Ultimate 3000 RSLCnano system (Thermo Scientific) connected in-line to a Q Exactive HF mass spectrometer (Thermo Scientific) equipped with a Nanospray Flex Ion Source (Thermo Scientific). Trapping was performed at 10 μL/min for 4 min in loading solvent [0.1% TFA in water/acetonitrile (98:2, vol/vol)] on a 20-mm trapping column [made in house, 100-μm i.d., 5-μm beads, C18 Reprosil-HD (Dr. Maisch)], and the sample was loaded on a 400-mm analytical column [made in house, 75-μm i.d., 1.9-μm beads C18 Reprosil-HD (Dr. Maisch)]. Peptides were eluted by a nonlinear increase from 2% to 56% solvent B [0.1% formic acid (FA) in water/acetonitrile (2:8, vol/vol)] over 140 min at a constant flow rate of 250 nL/min, followed by a 10-min wash reaching 99% solvent B and reequilibration with solvent A [0.1% FA in water/acetonitrile (98:2, vol/vol)]. The column temperature was kept constant at 50 °C in a column oven (CoControl 3.3.05; Sonation). The mass spectrometer was operated in data-dependent mode, automatically switching between MS and MS/MS acquisition for the 16 most abundant ion peaks per MS spectrum. Full-scan MS spectra (375–1,500 *m/z*) were acquired at a resolution of 60,000 in the orbitrap analyzer after accumulation to a target value of 3,000,000. The 16 most intense ions above a threshold value of 13,000 were isolated (window of 1.5 *m/z*) for fragmentation at a normalized collision energy of 28% after filling the trap at a target value of 100,000 for a maximum of 80 ms. MS/MS spectra (200–2,000 *m/z*) were acquired at a resolution of 15,000 in the orbitrap analyzer. The S-lens RF level was set at 55, and we excluded precursor ions with single and unassigned charge states from fragmentation selection.

From the MS/MS data in both LC runs, Mascot generic files (mgf) were created using Mascot Distiller software (version 2.5.1.0; Matrix Science Ltd.). When generating peak lists, grouping of spectra was performed with 0.005 *m/z* tolerance on the precursor ion, a maximum intermediate retention time of 30 s, and a maximum intermediate scan count of 5. A peak list was generated only when the MS/MS spectrum contained more than 10 peaks; no deisotoping was performed, and the relative signal to noise limit was set at 2. For both samples the generated peak lists were then searched with Mascot using the Mascot Daemon interface (version 2.5.1; Matrix Science Ltd.) against the human proteins in the UniProt database (database release version of January 2017 containing 20,246 human protein sequences). Spectra were first searched with semi-ArgC/P enzyme settings, allowing one missed cleavage. Heavy acetylation ($^{13}C_2D_3$) of lysine residues and carbamidomethylation of cysteine residues were set as fixed modifications, while oxidation of methionine residues was set as a variable modification. Mass tolerance of the precursor ions was set to 10 ppm (with Mascot's C13 option set to 1) and of fragment ions to 20 mDa. The instrument setting was set to ESI-QUAD. To allow identification and quantification of acetylated N-terminal peptides, a quantitation method with two different components was made defining light ($^{12}C_2H_3$) and heavy ($^{13}C_2D_3$) acetylation of peptide N termini as light and heavy exclusive modification groups, respectively. Only peptides that were ranked first and scored above the threshold score set at 99% confidence were retained. In a second search, peptides without N-terminal acetylation were identified using a similar search parameter set, including the cyclization of N-terminal glutamine residues to pyroglutamine residues as a variable modification. The false-discovery rate was calculated as described previously (6) and found to be 0.96%.

Identified peptides were quantified using the Mascot Distiller Toolbox version 2.3.2.0 (Matrix Science) in the precursor mode. The software tries to fit an ideal isotopic distribution on the experimental data based on the peptide average amino acid composition. This is followed by extraction of the Extracted Ion Chromatogram (XIC) signal of both peptide components (light and heavy) from the raw data. Ratios are calculated from the area below the light and heavy isotopic envelope of the corresponding peptide (integration method: trapezium; integration source: survey). To calculate this ratio value, a least squares fit to the component intensities from the different scans in the XIC peak was created. MS scans used for this ratio calculation are situated in the elution peak of the precursor determined by the Distiller software (XIC threshold 0.3, XIC smooth 1, maximum XIC width 250). To validate the calculated ratio, the SE on the least square fit must be below 0.16, and correlation coefficient of the isotopic envelope should be above 0.97.

For processing all MS data, the ms_lims software platform was used (7). During downstream analysis, peptides shorter than eight amino acids, peptides not starting at position 1 or 2 in the protein sequence, and nontryptic peptides were removed. Further selection for peptides that were reliably quantified led to a list of 402 N-terminal peptides that were successfully identified and quantified in both samples (Table S1). For each of these peptides, the degree of in vivo acetylation was calculated separately in both samples using the light/heavy (Ac/AcDC) ratio reported by the Mascot Distiller Toolbox by the equation Ac % = ratio (Ac/AcDC)/ratio (Ac/AcDC) + 1. In those cases where N-terminal peptides were identified and quantified multiple times, the median and SD of the acetylation degrees of the individual peptides was calculated.

The mass spectrometry proteomics data have been deposited in the ProteomeXchange Consortium via the PRIDE (8) partner repository with the dataset identifier PXD006856 (username: reviewer89589@ebi.ac.uk; password: LMHVncnM).

Purification of Ac-Actin and Non–Ac-actin. Ac-actin and non–Ac-actin were purified from HAP1 cells (Horizon Discovery) using a gelsolin-affinity purification protocol (9). *NAA80*-KO and wild-type HAP1 cells were grown in 15-cm-diameter plates (Corning) to 70% confluence in Iscove's Modified Dulbecco's Medium (Thermo Fisher Scientific) with the addition of 10% FBS and 1% penicillin/streptomycin. Cells were harvested and lysed using a glass homogenizer in binding buffer [10 mM Tris·HCl (pH 8.0), 5 mM $CaCl_2$, 1 mM ATP, 7 mM 2-mercaptoethanol] supplemented with cOmplete protease inhibitor mixture (Roche), 10 μg/mL leupeptin, and 1 mM phenylmethanesulfonyl fluoride (PMSF). Cell lysates were incubated overnight at 4 °C by gentle mixing with an affinity tag consisting of gelsolin subdomains 4–6, which binds actin in a Ca^{2+}-dependent manner. The lysates were centrifuged for 20 min at 200,000 × *g*, and the supernatant was incubated for 1 h with 2 mL nickel-nitrilotriacetic acid (Ni-NTA) resin (Qiagen), which binds the gelsolin–actin complex through an N-terminal polyhistidine affinity tag on the gelsolin fragment. The resin was washed with 10 column volumes of binding buffer with the addition of 100 mM KCl and 20 mM imidazole, which removes nonspecific binders, followed by five column volumes of binding buffer without $CaCl_2$. Actin was then eluted with 4 mL of binding buffer in which $CaCl_2$ was replaced by 1 mM EGTA. The released actin was polymerized for 1 h at 23 °C with the addition of 1 mM $MgCl_2$ and 100 mM KCl. The polymerized actin was then pelleted by centrifugation for 45 min at 370,000 × *g*, sheared using a glass homogenizer to break the pellet, and depolymerized through a 3-d dialysis against G-buffer [2 mM Tris·HCl (pH 8.0), 0.2 mM $CaCl_2$, 0.2 mM ATP], followed by centrifugation for 45 min at 370,000 × *g* to remove any actin that did not depolymerize.

Expression and Purification of Actin-Binding Proteins. Plasmids carrying the genes of mouse mDia1 (UniProt ID: O08808) and mDia2 (UniProt ID: Q9Z207) were a generous gift of Harry Higgs (Geisel School of Medicine at Dartmouth, Hanover, NH). The fragments encoding the constitutively active FH1–FH2 regions of both formins (mDia1 residues 549–1,255 and mDia2 residues 540–1,171) were amplified by PCR and cloned between the NdeI and BamHI sites of vector pCold (Clontech Laboratories). The cDNA of human gelsolin (UniProt ID: P06396) was purchased from Open Biosystems (GE Healthcare). The fragment encoding subdomains 4–6 (gelsolin residues 434–782) was amplified by PCR and cloned between the XhoI and EcoRI sites of vector pCold. All proteins cloned in the pCold vector were expressed in Rosetta (DE3) cells (Novagen) grown in Terrific Broth medium (for 1 L: 24 g yeast extract, 12 g tryptone, 4 mL glycerol, 0.17 M KH_2PO_4, 0.72 M K_2HPO_4) at 37 °C until the OD_{600} reached a value of 0.8 followed by 24 h at 15 °C in the presence of 0.3 mM IPTG. Cells were then harvested by centrifugation, resuspended in 50 mM Tris·HCl (pH 8.0), 500 mM NaCl, 5 mM imidazole, and 100 μM PMSF, and lysed using a Microfluidizer (Microfluidics Corporation). All the proteins were purified on a Ni-NTA affinity column according to the manufacturer's protocol (Qiagen). The mDia1 and mDia2 fragments were additionally purified through gel filtration in a SD200HL 26/600 column (GE Healthcare) in 20 mM Mes (pH 6.5) and 250 mM NaCl and a MonoS ion exchange column (GE Healthcare) in 20 mM Mes (pH 6.5) and a 100–1,000 mM NaCl gradient.

The cDNAs encoding for mouse *N*-WASP (UniProt IS: Q91YD9) and human profilin1 (UniProt: P07737) and profilin2 (UniProt: P35080) were purchased from ATCC. The fragment encoding for the C-terminal WCA region of *N*-WASP (residues 426–501), which is sufficient to activate the Arp2/3 complex, was amplified by PCR and cloned between the NdeI and EcoRI sites of vector pTYB12 (New England Biolabs). Profilin1 and profilin2 were cloned between the SapI and EcoRI sites of vector pTYB11 (New England Biolabs). The pTYB vectors encode for a chitin-binding domain, used for affinity purification, and an intein domain, used for self-cleavage and release of purified proteins after purification. The proteins cloned in pTYB vectors were expressed in BL21(DE3) cells (Invitrogen) and were grown in Terrific Broth medium at 37 °C until the OD_{600} reached a value of 1.5–2, followed by 16 h at 20 °C in the presence of 0.5 mM IPTG. Cells were harvested by centrifugation, resuspended in 20 mM Hepes (pH 7.5), 500 mM NaCl, 1 mM EDTA, and 100 μM PMSF, and lysed using a Microfluidizer. All proteins were purified on a chitin affinity column according to the manufacturer's protocol (New England Biolabs), followed by additional purification through a HiLoad 16/600 Superdex 75 gel-filtration column (GE Healthcare) in 20 mM Hepes (pH 7.5) and 100 mM NaCl. The Arp2/3 complex was purified from bovine brain as previously described (10).

All proteins used in this study were purified to homogeneity as confirmed by SDS/PAGE analysis (Fig. S7*A*).

Actin Polymerization and Depolymerization Assays. Ac-actin and non–Ac-actin were mixed in G-buffer with 6% α-actin labeled at Cys374 with pyrene iodoacetamide (pyrene-actin) to produce a stock of 6% pyrene-labeled actin. Actin polymerization was measured as the time course of the fluorescence increase resulting from the incorporation of pyrene-actin (excitation 365 nm, emission 407 nm) into filaments using a Cary Eclipse fluorescence spectrophotometer (Varian Medical Systems). All the actin assembly assays were conducted at 25 °C and were repeated three or more times, as indicated in Fig. 4. The polymerization of actin alone was carried out by mixing 4 μL of buffer alone with 200 μL of Mg–ATP–actin at 2 μM concentration (6% pyrene-labeled α-actin) in F-buffer [10 mM Tris (pH 8.0), 1 mM $MgCl_2$, 50 mM KCl, 1 mM EGTA, 0.2 mM ATP, 0.5 mM DTT, 0.1 mM NaN_3]. Data acquisition started 10 s after mixing. Polymerization assays

with actin assembly factors were carried out in the same manner, by mixing Mg–ATP–actin with 4 μL mDia1, mDia2, or Arp2/3 complex (with 100 nM *N*-WASP WCA). The concentration of mDia1 and mDia2 in the polymerization reaction varied from 10 to 50 nM and that of the Arp2/3 complex varied from 5 to 20 nM, as indicated in Fig. 4. Relative polymerization rates were calculated as the maximal slope of the polymerization curve between 0.1 and 0.4 of the maximum fluorescence divided by the maximal slope of the curve of actin alone.

Actin filament seeds were prepared by polymerizing 10 μM actin monomers in F-buffer for 2 h at 23 °C. The actin polymerized in this manner was then passed five times through a 27-gauge syringe needle to shear the actin filaments. The sheared filaments were then aliquoted into the precise volumes used in the experiments (to avoid multiple pipetting steps from a single seed stock, which shears the filaments) and were allowed to reanneal overnight. To load the filament seeds into the spectrophotometer cuvette, a one-time operation, we used 22.9-cm glass Pasteur pipettes (VWR), releasing gently to avoid filament shearing.

In filament depolymerization experiments the actin seeds were labeled, i.e., they consisted of 10% pyrene-labeled α-actin and 90% unlabeled cytoplasmic β/γ-actin. The depolymerization rate was then measured from the fluorescence decrease resulting from the dissociation of pyrene-labeled α-actin monomers from preassembled actin filament seeds diluted to 0.1 μM in F-buffer immediately before data acquisition. The depolymerization rates reported correspond to the maximal slope of the first 10% of the depolymerization curve, corresponding to the first 10% of the depolymerization decrease.

In filament elongation experiments the actin seeds were not labeled. In these experiments, 1.5 μM preassembled β/γ-actin filament seeds in F-buffer were mixed with 0.5 μM β/γ-actin monomers (6% pyrene-labeled α-actin), i.e., a monomer concentration below the critical concentration for monomer addition at the pointed end (0.6 μM) but above that of the barbed end (0.1 μM), such that monomer addition can occur only at the barbed end. Data acquisition started 10 s after mixing. Filament elongation rates correspond to the maximal slope of the first 10% of the polymerization curve resulting from the fluorescence increase due to the incorporation of pyrene-labeled actin monomers to the barbed ends of the β/γ-actin filament seeds. For barbed-end elongation experiments with mDia1 and profilin, the actin filament seeds were preincubated with 20 nM mDia1, whereas the actin monomers were preincubated with 1.5 μM profilin1 (or profilin2). The mDia1-preincubated filaments and profilin-preincubated monomers were then mixed, and elongation rates wer measured as above. All the measurements were done at 25 °C and were repeated at least three times.

G/F-Actin Ratio. For determining the G/F-actin ratios we used the G/F-actin In Vivo Biochem kit from Cytoskeleton, Inc., following the manufacturer's instructions. Briefly, 2×10^6 cells per cell line were washed briefly with 1 × PBS and then were harvested by scraping. Cells were resuspended in 750 μL prewarmed LAS1 buffer [50 mM Pipes (pH 6.9), 50 mM NaCl, 5 mM $MgCl_2$ 5 mM EGTA, 5% (vol/vol) glycerol, 0.1% Nonidet P-40, 0.1% Triton X-100, 0.1% Tween 20, 0.1% 2-mercapto-ethanol, 0.001% Antifoam C supplemented with 1 × protease inhibitor mixture (0.4 mM tosyl arginine methyl ester, 1.5 mM leupeptin, 1 mM pepstatin A, 1 M benzamidine) and 1 mM ATP] and subsequently were lysed using the EMBL cell cracker (ball size 8.010 mm) with 16 strokes. Cell debris was removed by centrifugation (400 × *g*, 5 min, RT), and 100 μL of cleared supernatant was transferred into an ultracentrifugation tube. F-actin was pelleted by ultracentrifugation (150,000 × *g*, 1 h, 4 °C). Supernatant (the G-actin fraction) was removed, and the F-actin–containing pellet was washed twice carefully with MilliQ water before being resuspended in 100 μL F-actin depolymerization buffer (1 μM cytochalasin D). F-actin samples were then incubated for 1 h on ice and were mixed every 20 min by pipetting. F-actin–positive control samples were prepared for each experiment adding 1 μM phalloidin to samples before ultracentrifugation for 10 min at RT. SDS loading buffer was added to the samples, and G/F-actin ratios were determined by SDS/PAGE and subsequent immunoblot analyses and densitometry using a pan-actin antibody.

IF. Cells grown on glass coverslips (Assistant) were fixed with 3% (wt/vol) paraformaldehyde (PFA) in 0.1 M phosphate buffer for 30 min and subsequently were permeabilized with methanol (−20 °C) for 10 min. Acetylated actins were detected by incubating cells with either Ac-β-actin or Ac-γ-actin antibodies for 2 h followed by Alexa594-conjugated secondary antibody (Jackson ImmunoResearch Laboratories) labeling for 1 h, and coverslips were mounted on a drop of ProLong Diamond antifade reagent containing DAPI (Molecular Probes). F-actin was detected by permeabilizing PFA-fixed cells with 0.2% Triton X-100 (in PBS) for 10 min and incubation with 100 nM of Rhodamine-phalloidin for 30 min.

Phalloidin-Based Phenotype Characterizations. Lamellipodia phenotype was identified in cells seeded at 70,000 cells/mL in 24-well plates, fixed ∼24 h after seeding in 3% PFA in cytoskeleton buffer (CB) [10 mM Mes (pH 6.1), 150 mM NaCl, 5 mM EGTA, 5 mM glucose, 5 mM $MgCl_2$], washed in CB, permeabilized in 0.1% Triton X-100 for 10 min, and stained with Rhodamine phalloidin or Phalloidin-Atto-647N for counting and confocal/STED, respectively. Cells at the edge of clusters were counted as either positive or negative for the presence of lamellipodia (mitotic cells were not considered, nor were lamellipodia on top of neighboring cells). The experiment was repeated three times, and at least 500 cells per cell line were counted in each independent repetition. Filopodia phenotype analysis was performed by seeding cells at 25,000–50,000 cells/mL in 48-well plates; cells were fixed ∼24 h after seeding in 3% PFA in 0.1 M phosphate buffer for 30 min, subsequently permeabilized with 0.1% Triton X-100 for 10 min, and stained with Rhodamine phalloidin. Filopodia were counted on isolated cells, and length measurements were done using ImageJ software (NIH).

Actin Repolymerization Assay in Cells. Complete depolymerization of F-actin was achieved by incubating cells with 500 nM LatA for 1 h at 37 °C. Cells were either fixed with PFA (control) or washed with culture medium to remove LatA and were further incubated in drug-free medium at 37 °C. Samples were taken every 2 min, fixed, permeabilized with 0.2% Triton X-100 (in PBS) for 10 min, and F-actin–probed with 500 nM phalloidin Atto 647N (STED microscopy) for 30 min.

Microscopy. Samples were examined using a Leica TCS SP8 STED 3× (Leica Microsystems) confocal laser microscope equipped with a 100×/1.4 NA HC PL APO STED white oil-immersion objective, 1 Airy unit pinhole aperture, and the appropriate filter combinations. Images were acquired with a 405-nm blue-diode (50 mW), white-light (470–670 nm lambda range, power ∼1.5 mW per line, pulsed supercontinuum), and 775-nm depletion (STED) lasers. Images were processed using Photoshop CS5 imaging software (Adobe Systems).

Sequence Alignment and Phylogenetic Analysis. Sequence alignments were generated by using the T-Coffee multiple sequence alignment tool (11). The alignment was arranged in Jalview with BLOSUM62 score color coding (purple tone showing the degree of conservation). For phylogenetic analysis, NAT6/NAA80 orthologs were identified using reciprocal BLASTP searches. Species representing crown eukaryotic groups (12, 13) in which NAT6 could not be identified were further investigated by analyzing the sequences of the actin isoforms by UniProt searches. Only complete and unfragmented actin isoform sequences were accepted and compared with NAA80's substrate specificity. The taxonomic tree was generated by using iTOL v3 (14).

1. Drazic A, Arnesen T (2017) [14C]-Acetyl-Coenzyme A-based in vitro N-terminal acetylation assay. *Methods Mol Biol* 1574:1–8.
2. Foyn H, Thompson PR, Arnesen T (2017) DTNB-based quantification of in vitro enzymatic N-terminal acetyltransferase activity. *Methods Mol Biol* 1574:9–15.
3. Vedeler A, Pryme IF, Hesketh JE (1991) The characterization of free, cytoskeletal and membrane-bound polysomes in Krebs II ascites and 3T3 cells. *Mol Cell Biochem* 100: 183–193.
4. Starheim KK, et al. (2009) Knockdown of human N alpha-terminal acetyltransferase complex C leads to p53-dependent apoptosis and aberrant human Arl8b localization. *Mol Cell Biol* 29:3569–3581.
5. Staes A, et al. (2017) Protease substrate profiling by N-terminal COFRADIC. *Methods Mol Biol* 1574:51–76.
6. Käll L, Storey JD, MacCoss MJ, Noble WS (2008) Assigning significance to peptides identified by tandem mass spectrometry using decoy databases. *J Proteome Res* 7: 29–34.
7. Helsens K, et al. (2010) ms_lims, a simple yet powerful open source laboratory information management system for MS-driven proteomics. *Proteomics* 10:1261–1264.
8. Vizcaíno JA, et al. (2016) 2016 update of the PRIDE database and its related tools. *Nucleic Acids Res* 44:D447–D456.
9. Ohki T, Ohno C, Oyama K, Mikhailenko SV, Ishiwata S (2009) Purification of cytoplasmic actin by affinity chromatography using the C-terminal half of gelsolin. *Biochem Biophys Res Commun* 383:146–150.
10. Boczkowska M, et al. (2008) X-ray scattering study of activated Arp2/3 complex with bound actin-WCA. *Structure* 16:695–704.
11. Notredame C, Higgins DG, Heringa J (2000) T-coffee: A novel method for fast and accurate multiple sequence alignment. *J Mol Biol* 302:205–217.
12. Hedges SB (2002) The origin and evolution of model organisms. *Nat Rev Genet* 3:838–849.
13. Baldauf SL (2003) The deep roots of eukaryotes. *Science* 300:1703–1706.
14. Letunic I, Bork P (2016) Interactive tree of life (iTOL) v3: An online tool for the display and annotation of phylogenetic and other trees. *Nucleic Acids Res* 44:W242–W245.

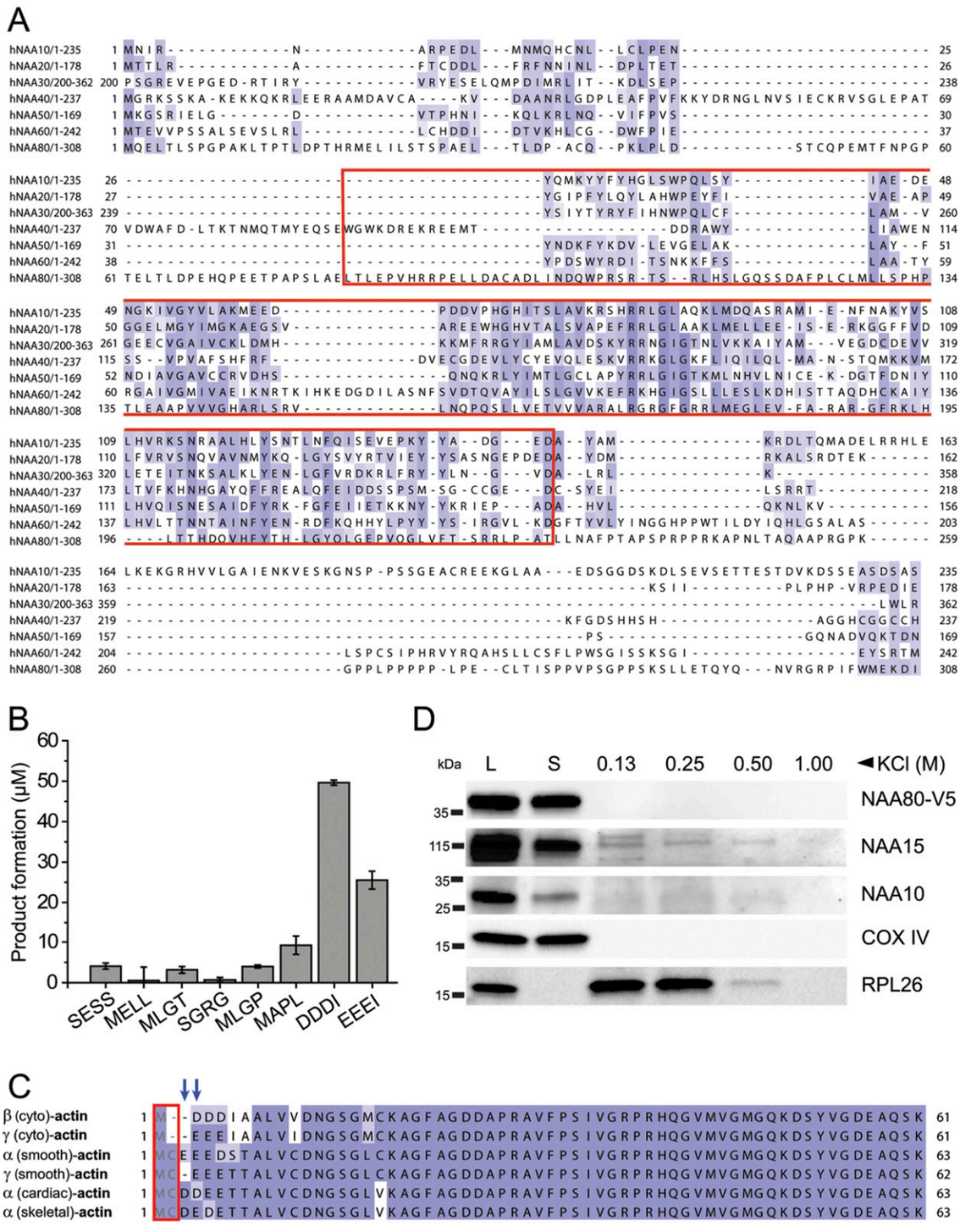

Fig. S1. NAA80 is a NAT specifically targeting acidic N termini. (*A*) Sequence alignment of the catalytic subunits (NAA10–NAA60 and NAA80) of the known human NATs (NatA–NatF, and NatH). Highlighted in the red box is the GNAT-fold for NAA80 according to Prosite (1). (*B*) DTNB-based Nt-acetylation activity assay using recombinantly purified MBP-NAA80 and selected peptides (*Materials and Methods*). The peptides represent typical substrates of the six characterized NATs [SESS (NatA); SGRG (NatD); MELL (NatB); MLGT (NatC); MLGP (NatE); MAPL (NatF)] as well as DDDI and EEEI, representing processed β- and γ-actin, respectively. For a detailed list of peptide sequences and their origin, see Table S3. Data are shown are the means ± SD of at least three independent experiments. (*C*) Sequence alignment of the first 61–63 amino acids of the six human mature actin isoforms generated as in *A*. Of note, methionines and/or cysteines at the second position (highlighted in gray in the red box) are removed before Nt-acetylation (blue arrows) of newly formed acidic N termini. (*D*) Polysome isolation from NAA80-V5–transfected HeLa cells via ultracentrifugation. Proteins bound to ribosomes were washed off by increasing KCl concentrations. NAA15 and NAA10 are known to be partly ribosome associated (2). COX IV is a mitochondrial protein and therefore does not bind to ribosomes. RPL26 is the ribosomal marker and serves as a positive control. NAA80-V5 does not bind to ribosomes, suggesting that it acts posttranslationally. L, lysate (input); S, supernatant after the first ultracentrifugation step (*Materials and Methods*). Shown is one representative experiment of three independent experiments performed.

1. de Castro E, et al. (2006) ScanProsite: Detection of PROSITE signature matches and ProRule-associated functional and structural residues in proteins. *Nucleic Acids Res* 34:W362–W365.
2. Arnesen T, et al. (2005) Identification and characterization of the human ARD1-NATH protein acetyltransferase complex. *Biochem J* 386:433–443.

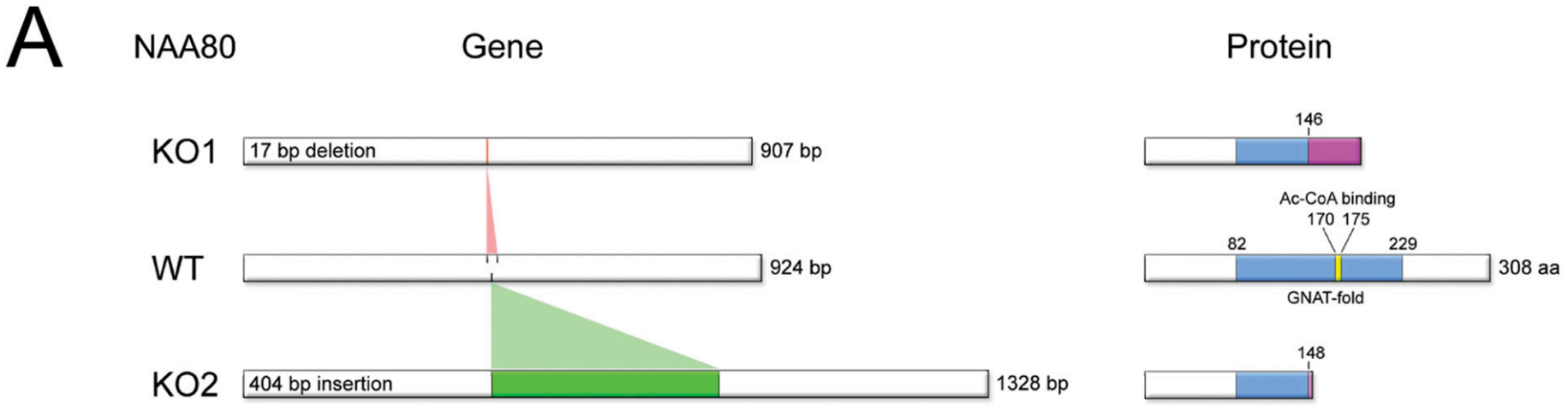

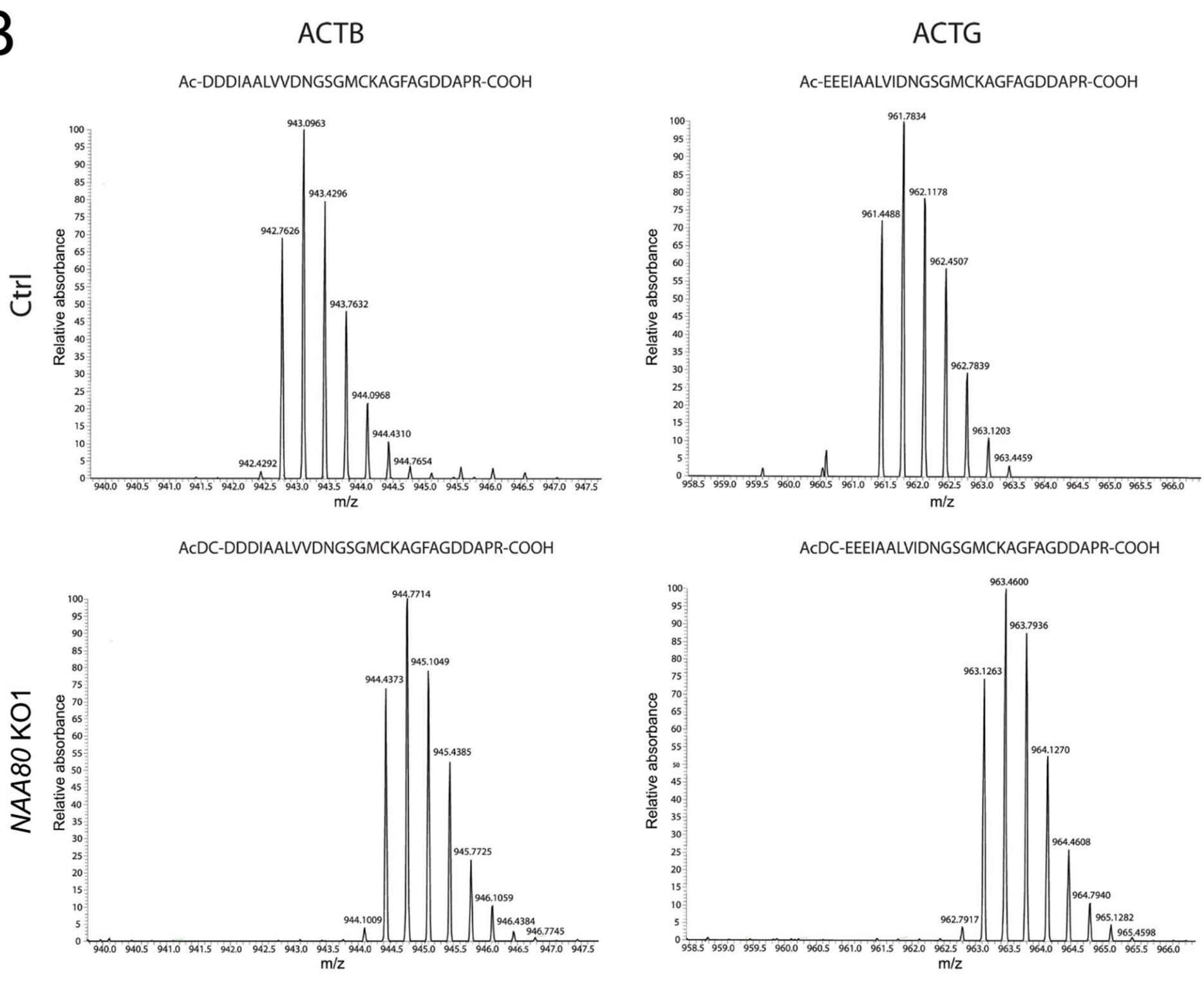

Fig. S2. Actin is not Nt-acetylated in *NAA80*-KO cells. (*A*, *Left*) *NAA80* KO1 cells were generated by deleting 17 bp from exon 2 (red), and *NAA80* KO2 was generated by inserting 404 bp into exon 2 (green) of the *NAA80* gene. (*Right*) The putative gene product of *NAA80* KO1 consists of a 193-aa protein, and the putative gene product of *NAA80* KO2 consists of a 151-aa protein. Both KO gene products lack the crucial Ac-CoA binding motif. Red, deletion; green, insertion; blue, catalytic GNAT domain; purple, newly translated amino acid divergent from wild-type *NAA80*; yellow, Ac-CoA binding motif. (*B*) Representative mass spectra of β-actin's (ACTB) and γ-actin's (ACTG) Nt-acetylation status from HAP1 control (Ctrl) (*Upper*) and *NAA80* KO1 (*Lower*) cells determined by SCX enrichment and subsequent mass spectrometry analysis. In control cells, only the in vivo-acetylated N-terminal peptides were observed (Ac-DDDIAALVVDNGSGMC < Cmm > K<AcDC > AGFAGDDAPR-COOH, 942.76 *m/z*, 3+ for ACTB and Ac-EEEIAALVIDNGSGMC < Cmm > K<AcDC > AGFAGDDAPR-COOH, 961.45 *m/z*, 3+ for ACTG). In NAA80 KO1 cells, only the in vitro-acetylated forms were detected (AcDC-DDDIAALVVDNGSGMC < Cmm > K<AcDC > AGFAGDDAPR-COOH, 944.44 *m/z*, 3+ for ACTB and AcDC-EEEIAALVIDNGSGMC < Cmm > K<AcD3C13 > AGFAGDDAPR-COOH, 963.13 *m/z*, 3+ for ACTG). Ac, acetyl; AcDC, $^{13}C_2D_3$-acetyl; Cmm, carbamidomethyl.

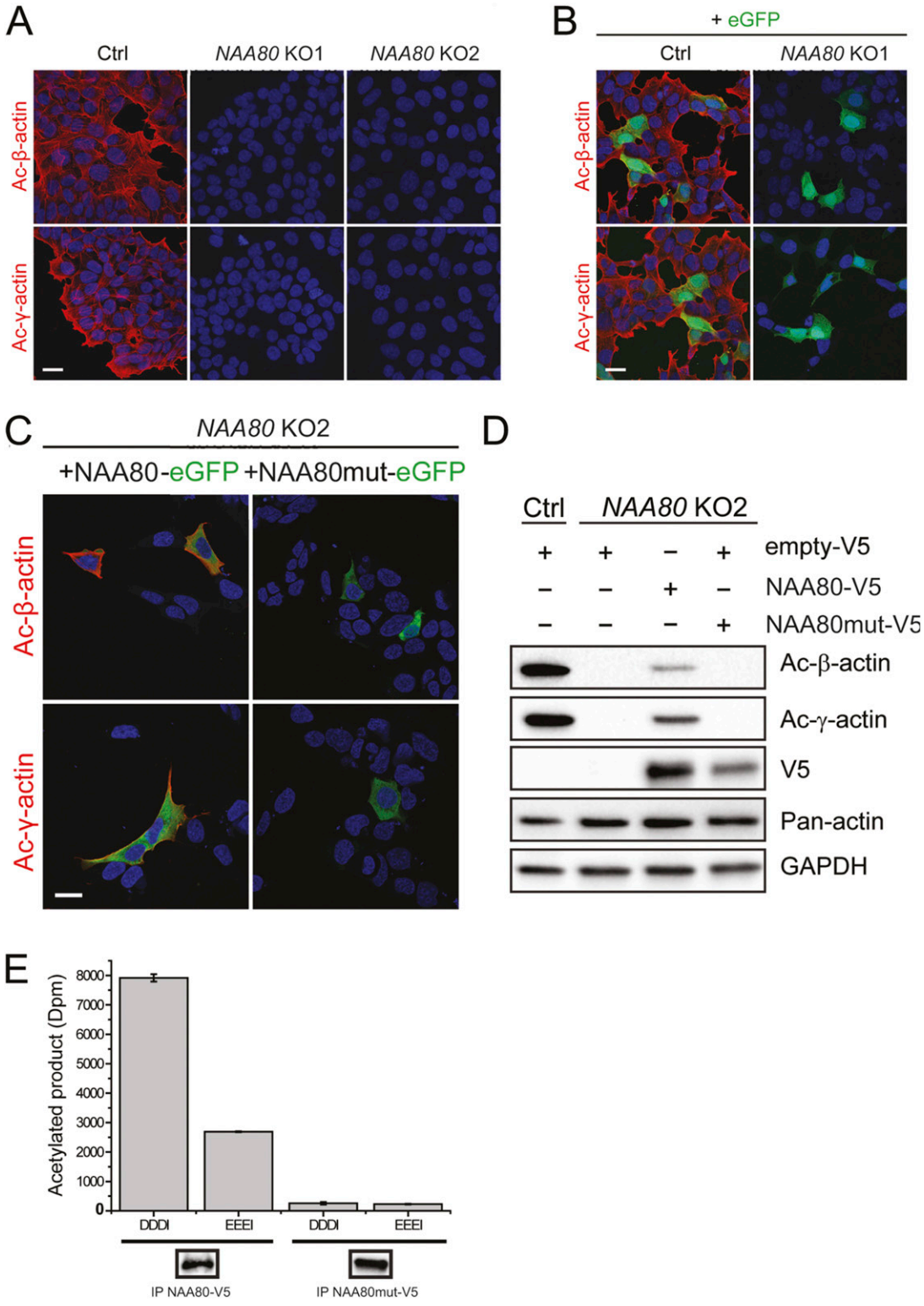

Fig. S3. Actin Nt-acetylation depends on NAA80's catalytic activity. (*A*) HAP1 control, *NAA80* KO1, and *NAA80* KO2 cells were stained with Ac-β– and Ac-γ-actin–specific antibodies and analyzed by IF, confirming that actin is not Nt-acetylated in the *NAA80*-KO cells. (*B*) Control and *NAA80* KO1 cells transfected with empty eGFP plasmid show no actin Nt-acetylation. (*C*) *NAA80* KO2 cells were transfected with wild-type NAA80-eGFP or NAA80mut-eGFP. Wild-type NAA80-eGFP–transfected cells, but not NAA80mut-eGFP–transfected cells, show reacetylation of the actin N terminus. (Scale bars, 20 μm.) (*D*) Immunoblot analysis of HAP1 control and *NAA80* KO2 cells transfected with empty V5 plasmid, wild-type NAA80-V5, or NAA80mut-V5. The samples were probed with Ac-β– and Ac-γ-actin–specific antibodies and with pan-actin-, V5-, and GAPDH-specific antibodies. (*E*) [^{14}C]-Ac-CoA–based activity assay with immunoprecipitated wild-type NAA80-V5 and the catalytically dead mutant NAA80mut-V5 tested toward the NAA80 substrates DDDI and EEEI. Data are shown as the means ± SD of at least three independent experiments.

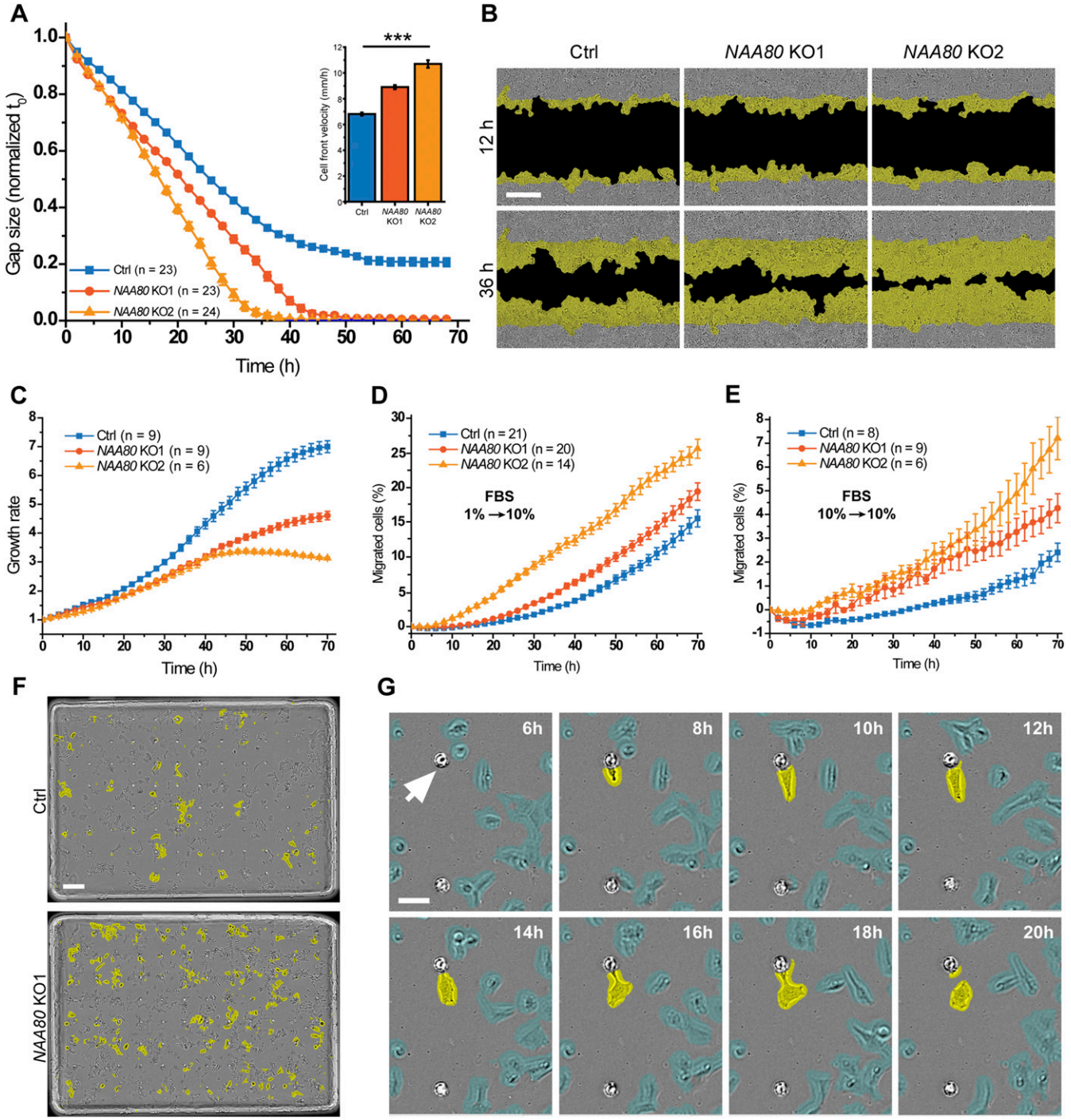

Fig. S4. *NAA80*-KO cells have increased migration. (*A*) Relative gap widths per time from a scratch in a wound-healing analysis monitored by the IncuCyte ZOOM system. (*Inset*) Cell-front velocities. ***$P < 0.001$, Student's *t* test ($n \geq 23$). (*B*) Representative images from the experiment in *A* at 12 h and 36 h after scratching. Yellow mask: cells that have migrated into the gap; black mask: remaining wound area. (Scale bar, 300 μm.) (*C*) Growth rates were measured in the chemotaxis assay (Fig. 2) to correct for proliferation differences between the cell lines. Data are the sum of the cell-covered area in the top and bottom chambers in control wells (top and bottom chambers containing cell culture medium with 10% FBS) and are expressed relative to t_0. (*D* and *E*) Chemotaxis (*D*) and random migration (*E*) of HAP1 control and *NAA80*-KO cells as the percentage of cells in the top chamber at t_0 and normalized to growth rates in *C*. Data shown here for control and *NAA80* KO1 cells are from Fig. 2 *D* and *E*. (*F*) Representative images of the chemotaxis assay indicating the amount of migrated cells after 44 h. (Scale bar, 200 μm.) (*G*) Single-cell movement through a pore (arrow) monitored in the chemotaxis assay shown for the *NAA80* KO1 experiment. Images are shown with the bottom side (10% FBS, attractant side) in focus. Yellow highlights cells on the bottom side of the transparent membrane; turquoise highlights cells on the top side. (Scale bar, 50 μm.) Shown are the means ± SEM of $n \geq 6$ replicates.

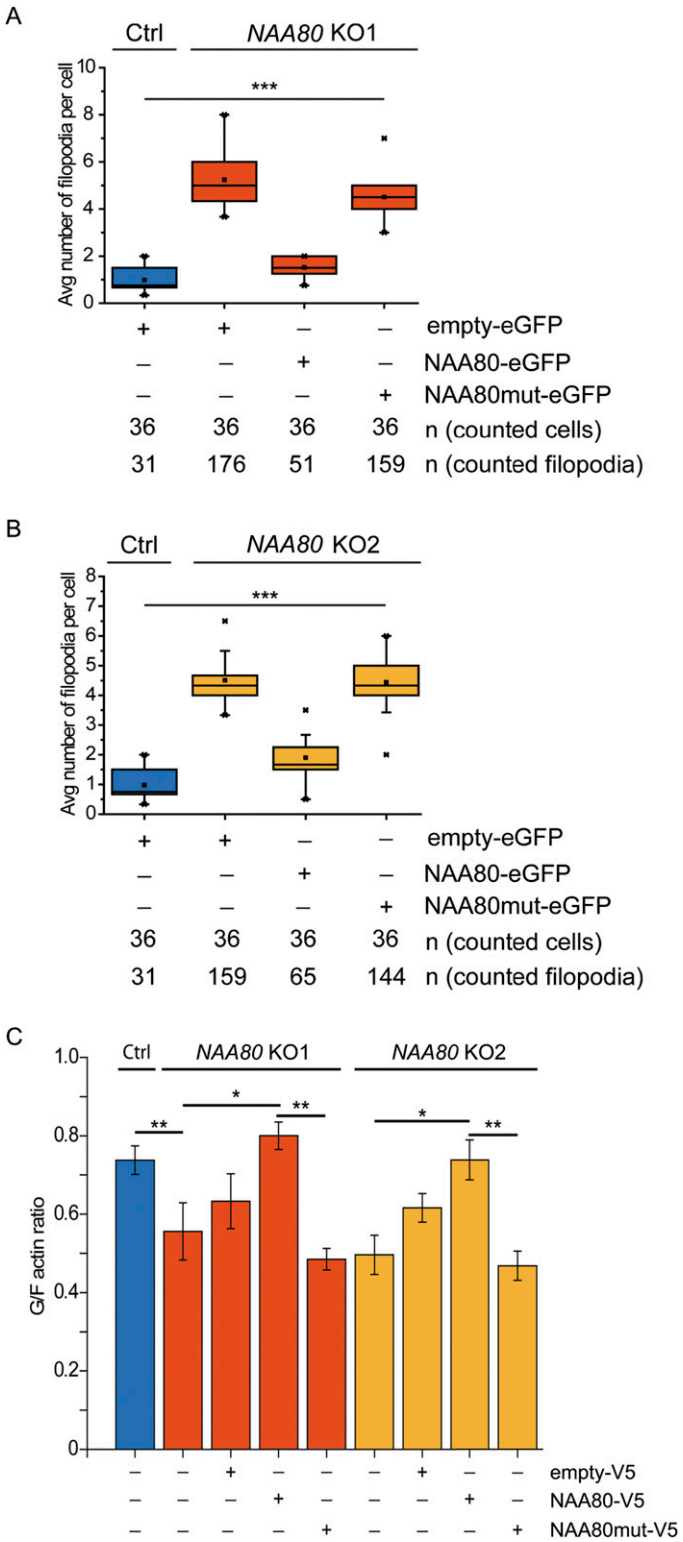

Fig. S5. NAA80 expression rescues actin phenotypes in *NAA80*-KO cells. Rescue of the protrusion phenotype by NAA80 expression. (*A* and *B*) Quantification of filopodia per cell in *NAA80* KO1 (F-actin) (*A*) and *NAA80* KO2 (G-actin) (*B*) cells. (*C*) G/F-actin ratios from HAP1 control (blue bar), *NAA80* KO1 (orange bars), and *NAA80* KO2 (light-orange bars) cells determined by immunoblot and subsequent densitometry analyses. Cells were either untreated (no transfection) or transfected with empty V5 plasmid, wild-type NAA80-V5, or NAA80mut-V5 for 48 h. $*P \leq 0.05$; $**P \leq 0.01$; $***P \leq 0.001$, Student's *t* test. Data are shown as the means ± SD of two to four independent experiments.

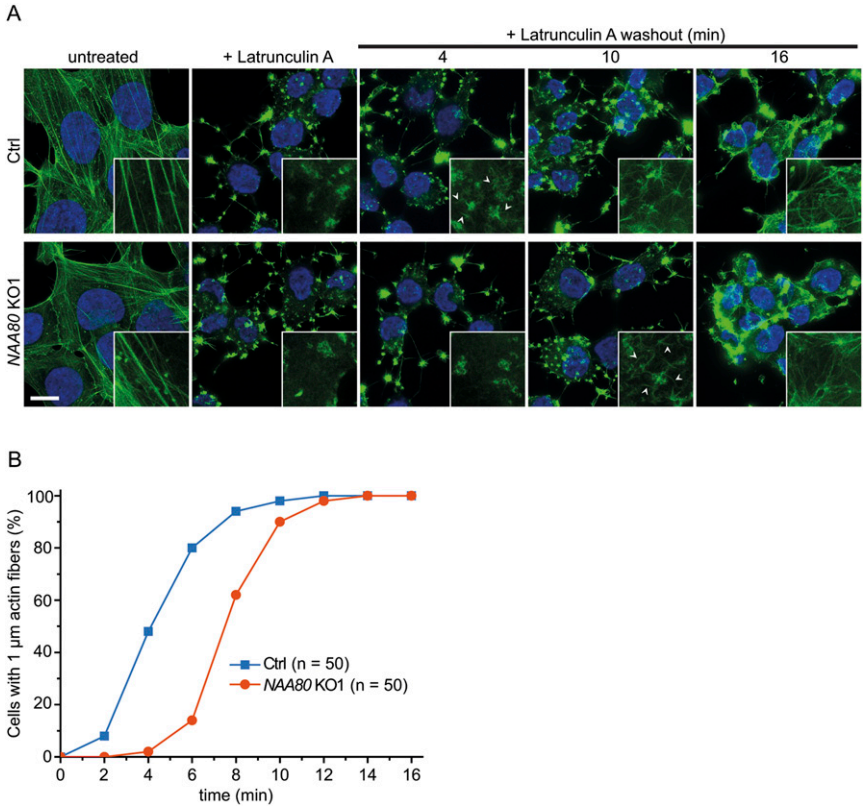

Fig. S6. Impaired repolymerization rates in *NAA80*-KO cells: The time-dependent actin fiber repolymerization rate is decreased in *NAA80*-KO cells. (*A*) HAP1 control (Ctrl) and *NAA80* KO1 cells were treated with LatA for 60 min, resulting in complete depolymerization of the actin cytoskeleton. Removing LatA initiates the fiber repolymerization (monitored by phalloidin Atto 647N staining for STED microscopy) of samples taken at 2-min intervals (*Insets*, arrowheads). Shown are representative experiments from $n = 4$. (Scale bar, 10 µm.) (*B*) Quantification of cells containing actin fibers in the experiment in *A* ($n = 50$ cells per time point). Actin filament formation was observed after 2 min in HAP1 control (Ctrl) cells and after 6 min in *NAA80*-KO cells.

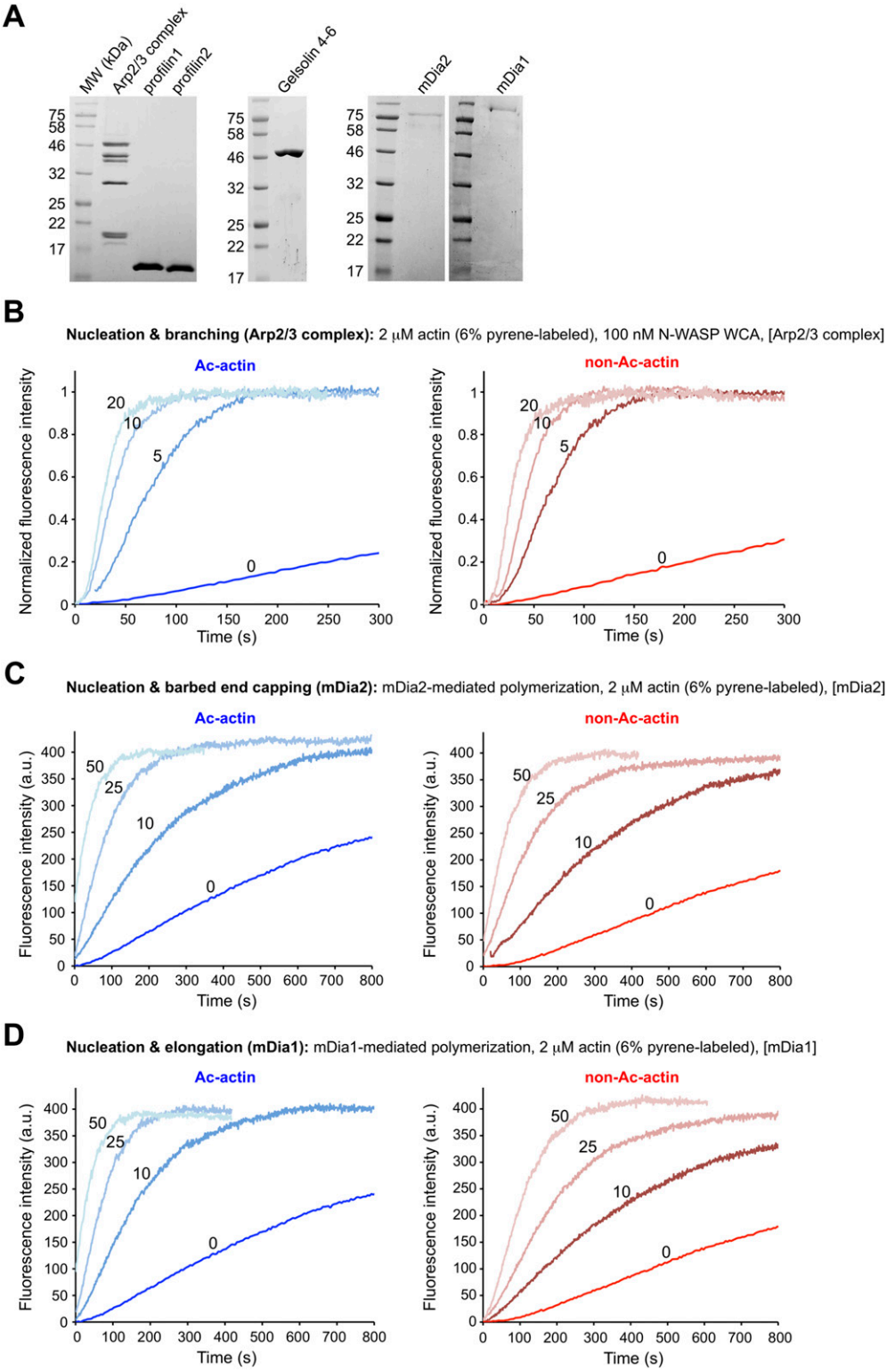

Fig. S7. Effect of Nt-acetylation on actin assembly in vitro. (*A*) SDS/PAGE analysis of the proteins produced for biochemical studies, including Arp2/3 complex purified from bovine brain tissue, recombinant profilin1 and profilin2, the gelsolin construct consisting of domains 4–6 and used in affinity purification of actin, and the FH1–FH2 fragments of mDia1 and mDia2. (*B*) Time course of actin polymerization (6% pyrene-labeled) as a function of Arp2/3 complex concentration and ± Nt-acetylation. Detailed experimental conditions for each panel are given in the figure and in *Materials and Methods*. (*C*) Time course of actin polymerization (6% pyrene-labeled) ± Nt-acetylation as a function of mDia2 concentration. (*D*) Time course of actin polymerization (6% pyrene-labeled) ± Nt-acetylation as a function of mDia1 concentration.

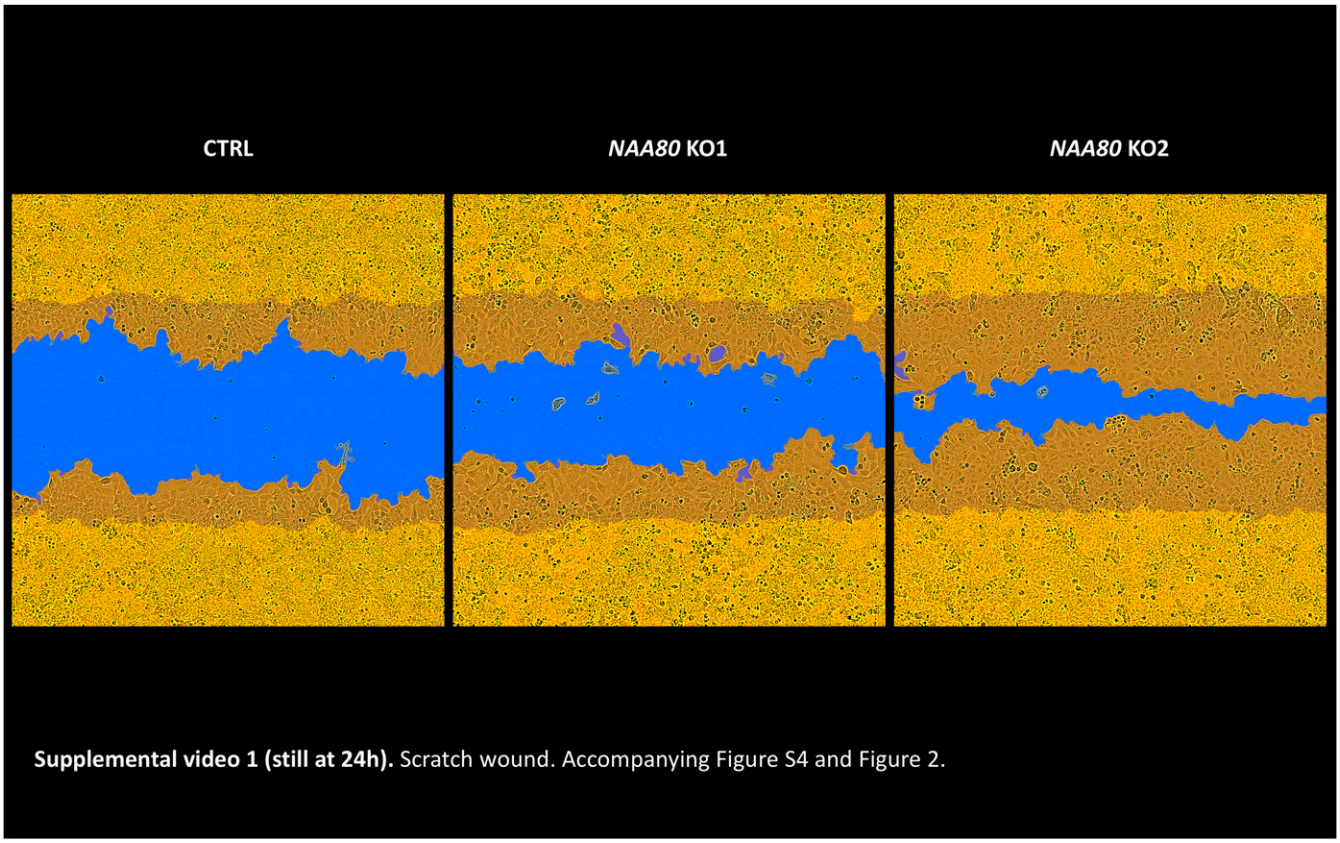

Movie S1. *NAA80*-KO cells have increased wound-healing capacity. Time-lapse video of the scratch wound assay shown in Fig. S4 *A* and *B*. HAP1 control (CTRL) cells and NAA80-KO cells (*NAA80* KO1 and *NAA80* KO2) were seeded in 96-well ImageLock plates (Essen BioScience) (200 μL of 40,000 cells/mL). Imaging and processing was performed on an IncuCyte ZOOM system.

Movie S1

Other Supporting Information Files

Table S1 (DOCX)
Table S2 (DOCX)
Table S3 (DOCX)